



Space Weather

RESEARCH ARTICLE

10.1029/2020SW002479

Key Points:

- Fluxes of energetic electrons (>200 keV) in SAA region are larger in the nighttime than the morning during geomagnetically quiet times
- The day-night difference of energetic electrons in SAA region depends not only on the electron energy but also on the geomagnetic conditions
- Enhanced geomagnetic activities increase the energetic electrons in morning and hence weaken their day-night difference in the SAA region

Correspondence to:

L. Y. Li,
lyli_ssri@buaa.edu.cn

Citation:

Li, L. Y., Zhou, S. P., Wei, S. H., Yang, J. Y., Sauvaud, J. A., & Berthelier, J. J. (2020). The day-night difference and geomagnetic activity variation of energetic electron fluxes in region of South Atlantic anomaly. *Space Weather*, 18, e2020SW002479. <https://doi.org/10.1029/2020SW002479>

Received 15 FEB 2020

Accepted 28 APR 2020

Accepted article online 16 MAY 2020

The Day-Night Difference and Geomagnetic Activity Variation of Energetic Electron Fluxes in Region of South Atlantic Anomaly

L. Y. Li^{1,2} , S. P. Zhou¹, S. H. Wei¹, J. Y. Yang^{1,2} , J. A. Sauvaud³ , and J. J. Berthelier⁴

¹School of Space and Environment, Beihang University, Beijing, China, ²Key Laboratory of Space Environment Monitoring and Information Processing of MIIT, Beijing, China, ³IRAP-UMR5277, CNRS-University of Toulouse, Toulouse, France, ⁴LATMOS/IPSL, UPMC, Paris, France

Abstract Utilizing the DEMETER observations at 670 km, we examined the day-night difference of energetic electrons (100–800 keV) in the South Atlantic Anomaly (SAA) region and their dependence on geomagnetic activities in different seasons. Under geomagnetically quiet conditions, the fluxes of higher-energy electrons (>200 keV) in the dusk and midnight (MLT ~19–24 hr) are usually larger than those in the morning (MLT ~8–12 hr) in the core region of the SAA ($-50 \leq \lambda \leq -20$ deg) during the northern and southern summers (21 March 2007 to 23 September 2007 and 23 September 2007 to 21 March 2008). The day-night difference of energetic electrons in SAA region depends not only on the electron energy but also on the geomagnetic activity levels. Enhanced geomagnetic activities increase the energetic electrons in morning and hence weaken their day-night difference in the SAA region.

1. Introduction

South Atlantic Anomaly (SAA) leads to particular disturbances in space environments over the Earth. In the SAA region, the remarkable decrease in geomagnetic field allows the trapped high-energy protons and electrons in the inner radiation belt to bounce to lower altitudes and thus generate radiation hazards to the spacecrafts and astronauts in low Earth orbits (Baker et al., 2018; Heirtzler, 2002; Ye et al., 2017; Zou et al., 2011, 2015). Under different geomagnetic conditions, cosmic ray albedo neutron decay (CRAND) is a relatively constant source of the 100-keV electrons in the region of $L < 1.3$ (Li, Selesnick, et al., 2017; Selesnick, 2015; Zhang et al., 2019). Moreover, the large-scale convection electric fields can cause energetic electron injections or radial diffusion into the inner radiation belt during active times (Selesnick et al., 2016).

Besides energetic particles, there are also dense neutral atmospheric compositions and cold plasmas in the SAA region at ionospheric altitudes (<800 km). Thus, energetic particles experience collisions with ambient cold plasmas and neutral compositions (Li et al., 2015; Selesnick, 2012). Satellite observations indicate that the density of cold plasmas in the nighttime is much less than the daytime in the SAA region (Horvath & Lovell, 2009; Li et al., 2011). However, no one knows whether the radiation environments of energetic particles have a remarkable day-night difference in SAA region. Here, we examined the day-night difference of energetic electron fluxes in SAA region and their dependence on geomagnetic activities in different seasons.

2. Data Source

During a tropic year (21 March 2007 to 21 March 2008), the Detection of Electro-Magnetic Emissions Transmitted from Earthquake Regions (DEMETER) satellite moved in a sun-synchronous circular orbit at ~670 km. The local times (LT) of the equatorial crossings by DEMETER are 10:30 a.m. and 10:30 p.m., respectively. The Instrument for Detecting Particles (IDP) on board DEMETER mainly measures the 70-keV to 2.54-MeV electrons (Sauvaud et al., 2006). The thermal plasma analyzer (Instrument d'Analyse du Plasma [IAP]) mainly records the number density and temperature ($\sim 10^2$ to 5×10^3 K) of ambient cold ions (O^+ , H^+ , and He^+) (Berthelier et al., 2006).

3. Spatial Range of SAA and Motion Periods of Charged Particles at 670 km

Since the spatial range of the SAA region is different at different altitudes, we showed the SAA region roughly through global distribution of magnetic field strength (B) at ~670 km. B was obtained from the

©2020. The Authors.

This is an open access article under the terms of the Creative Commons Attribution License, which permits use, distribution and reproduction in any medium, provided the original work is properly cited.

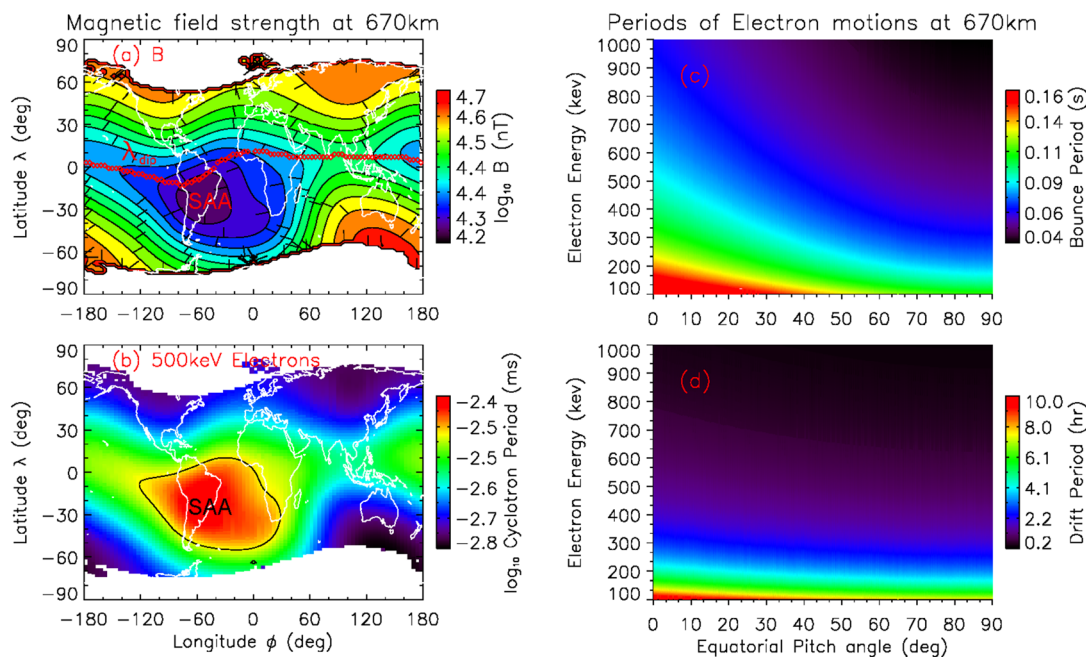


Figure 1. (a) Global distribution of magnetic field strength (B). (b–d) Motion periods of energetic electrons at 670 km. λ_{dip} is the magnetic dip equator (red diamonds). The South Atlantic Anomaly (SAA) region is marked out by the closed red curves.

mission center of DEMETER, and it was calculated with the model of International Geomagnetic Reference Field (IGRF). Based on the magnetic field strength (B) and the motion equations of charged particles (Lyons & Williams, 1984), we estimated the cyclotron, bounce, and drift periods of energetic electrons at 670 km.

Figure 1 shows the global distribution of magnetic field strength (B) and the motion periods of energetic electrons (100–1,000 keV) at 670 km. $B \leq 10^{4.3}$ nT in the SAA region ($-120 \leq \phi < 20$ deg, and $-60 < \lambda \leq 0$ deg), and the cyclotron period of energetic electrons is the maximum there (inside the closed red curve in Figure 1b). At 670 km, the bounce periods of energetic electrons are about 0.04 to 0.2 s, while their bounce-averaged drift periods are about 0.3 to 11 hr.

4. Day-Night Difference of Energetic Electrons in SAA Region During Quiet Times

Figures 2–5 show the differential fluxes of the 100 to 800 keV electrons in SAA region during geomagnetically quiet times ($K_p < 3$ and $Dst > -30$ nT and $AE < 200$ nT). The electron fluxes were observed by DEMETER around the vernal equinox (18 March), summer solstice (06 June), autumnal equinox (10 September), and winter solstice (15 December) in 2007. The curves with asterisks denote the electron fluxes in the morning (magnetic local time [MLT] ~ 8.5 –10.5 hr), while the curves with squares denote that in the nighttime (MLT ~ 22 –22.9 hr).

In the SAA region ($-50 < \phi < -20$ deg, and $-60 \leq \lambda \leq 0$ deg), the fluxes of different-energy electrons display different day-night asymmetries. The fluxes of lower-energy electrons ($E < 200$ keV) in morning are nearly comparable to those in nighttime, whereas the fluxes of higher-energy electrons ($E > 200$ keV) in nighttime are significantly larger than those in morning in all seasons under geomagnetically quiet times. The day-night differences of the higher-energy electrons are the most prominent near the core region of the SAA ($-50 \leq \lambda \leq -20$ deg). The large day-night difference of the higher-energy electrons indicates that the low-orbit satellites encounter more high-energy electrons in the SAA region in the nighttime than the daytime in different seasons during quiet times.

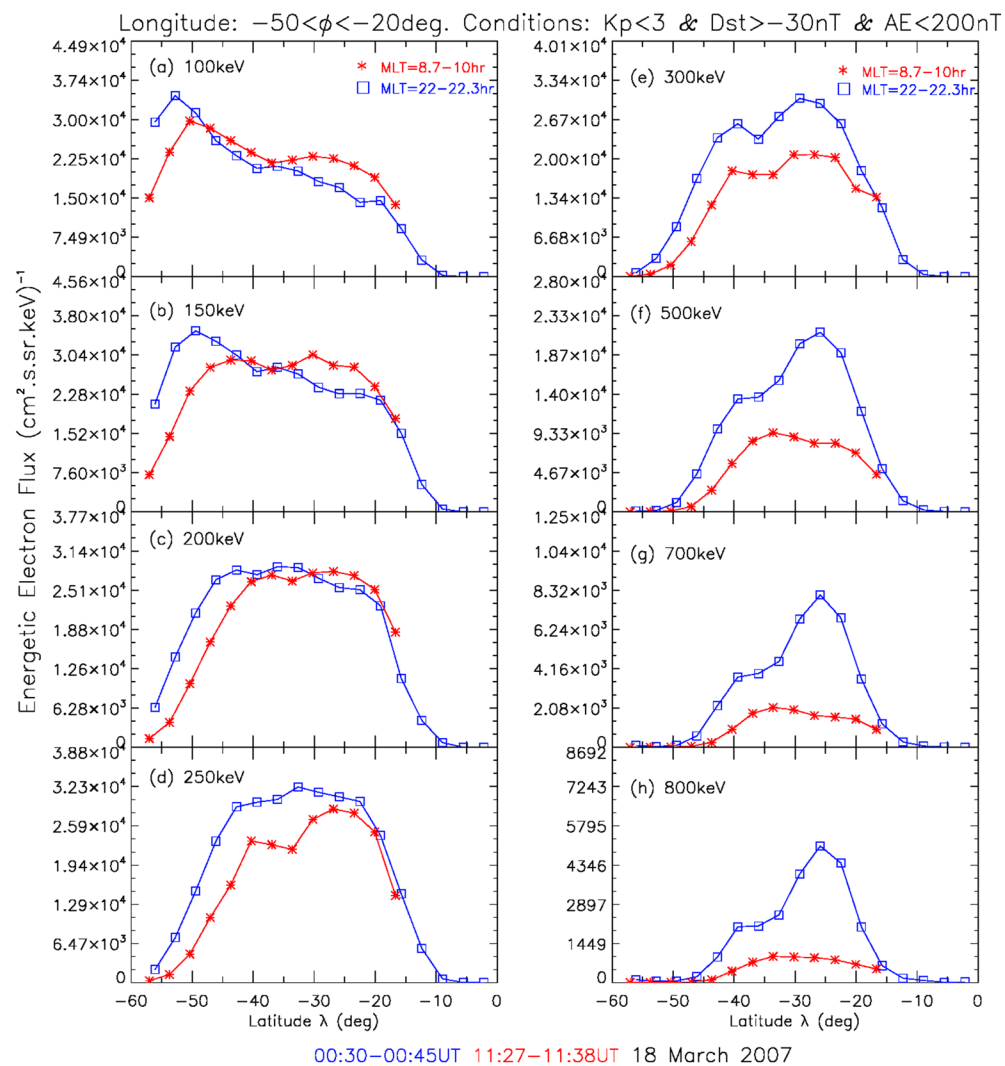


Figure 2. The differential fluxes of energetic electrons in South Atlantic Anomaly (SAA) region around the vernal equinox (18 March 2007) during geomagnetically quiet times. The fluxes of lower-energy electrons (<200 keV) in morning are comparable to those in nighttime, whereas those of higher-energy electrons (>200 keV) are significantly larger in the nighttime than in the morning.

The day-night difference of energetic electrons in the SAA region depends on the electron energy. Although the flux of the 200 keV electrons has also significant day-night difference around the solstices (06 June and 15 December), their flux becomes comparable around the equinoxes (18 March and 10 September). Similarly, the fluxes of the <200-keV electrons are also highly changed in different seasons. These observations indicate that the 200-keV and lower-energy electrons are more easily changed by a few of season-dependent factors (e.g., geomagnetic activities).

In order to examine the effect of seasonal changes on energetic electrons in SAA region, we selected the energetic electron data observed by DEMETER/IDP during the northern and southern summers (21 March 2007 to 23 September 2007 and 23 September 2007 to 21 March 2008), and then calculated the semiannually averaged electron fluxes within each grid of longitude and latitude ($2^\circ \times 1^\circ$) in daytime and nighttime. Figure 6 displays the global distribution of the semiannually averaged fluxes of the 500-keV electrons and their day-night differences under geomagnetically quiet conditions ($K_p < 3$ and $Dst > -30$ nT and $AE < 200$ nT). The day-night difference is equal to the nighttime flux minus the daytime one in the same grid (Panels c and f).

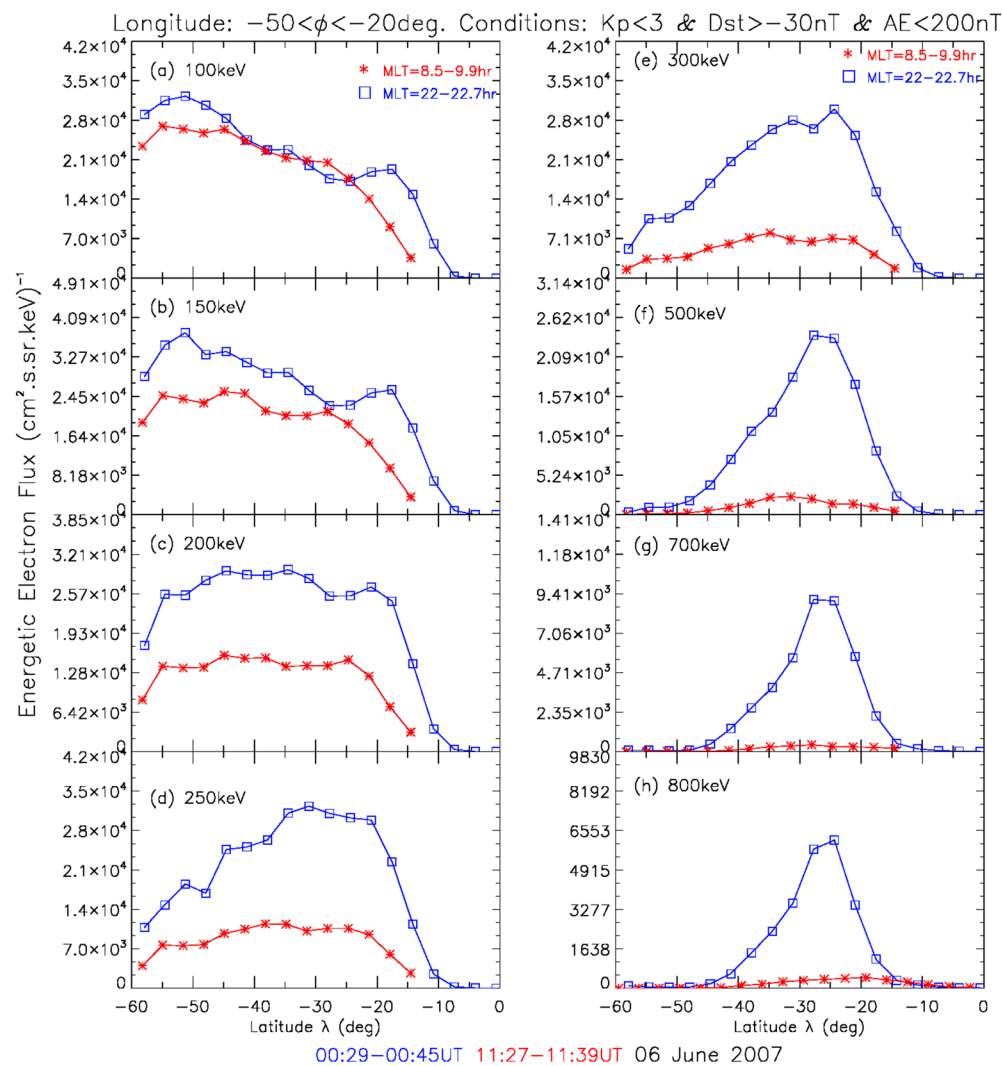


Figure 3. Similar to Figure 2, but around the summer solstice (06 June 2007) during quiet times.

In the core region of the SAA ($-50 \leq \lambda \leq -20$ deg, and $-80 \leq \varphi \leq 10$ deg), the day-night difference of the 500-keV electron fluxes is greater than 1.0×10^3 ($\text{cm}^2 \cdot \text{s} \cdot \text{sr} \cdot \text{keV}$) $^{-1}$ during the northern and southern summers. Similarly, the fluxes of other higher-energy electrons (e.g., 300 and 700 keV) have significant day-night differences in the core region of the SAA. These statistical results demonstrate that the fluxes of higher-energy electrons (>200 keV) in SAA region in nighttime are usually larger than those in morning.

Moreover, we also examined the global distributions of the semiannual averaged fluxes of lower-energy electrons (<200 keV) in morning and nighttime during the northern and southern summers. However, the fluxes of the lower-energy electrons have no significant day-night difference in the core region of the SAA during quiet times. The different local time distributions of energetic electrons suggest that different-energy electrons experience different dynamic processes at 670 km.

5. Discussions

5.1. Effect of Collisions With Cold Plasma Species and Neutral Compositions

During quiet times, the day-low and night-high electron fluxes are opposite to the day-night difference of plasma density in the SAA region. The density of cold ambient electrons (~eV) in the daytime is higher by one order of magnitude than the nighttime in the SAA region (Li et al., 2011). Therefore, energetic

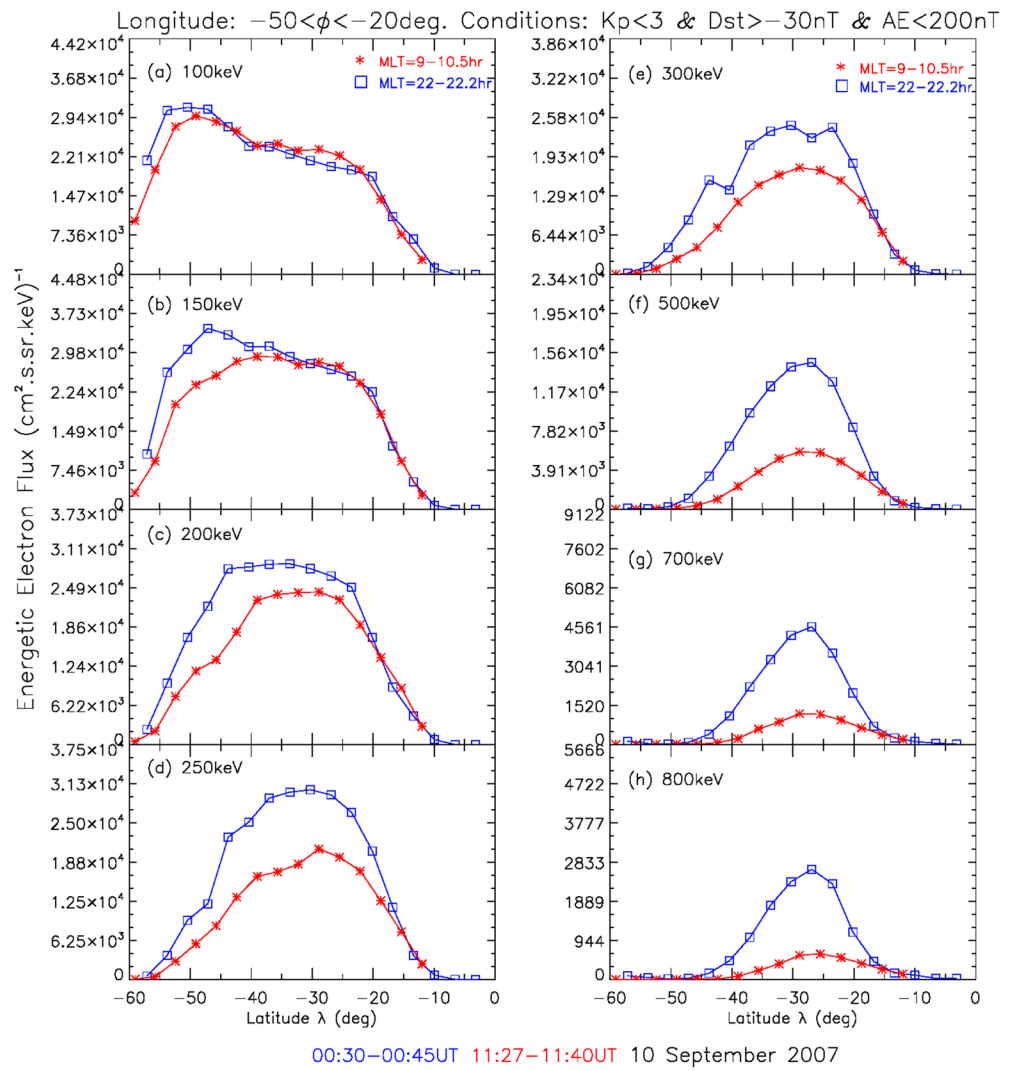


Figure 4. Similar to Figure 2, but around the autumnal equinox (10 September 2007) during quiet times.

electrons probably experience loss because of collisions with cold plasma species and neutral atmospheric compositions at 670 km. The pitch angle diffusion coefficient of energetic electrons induced by Coulomb collision is expressed as (Selesnick, 2012)

$$D_{xx} = \frac{2\pi r_e^3 m^3 c^4 y^2 \gamma}{p^3 x^3} \left\langle \left(\frac{B_0}{B} - y^2 \right) \left[n_e \lambda_e + \sum_i n_i Q_i \Delta \lambda + \sum_j n_j Z_j^2 \lambda_{nj} \right] \right\rangle, \quad (1)$$

where $r_e = e^2/(4\pi\epsilon_0 mc^2)$ is the electron gyroradius (e is the elementary charge), $y^2 = 1 - x^2 = \sin^2 \alpha_0$, and α_0 is the electron pitch angle. B and B_0 are the local and equatorial magnetic field strengths, respectively. n_e is the number density of ambient cold electrons, and $n_e \sim [e^-]$. Coulomb logarithm $\lambda_e = \ln\left(\frac{mv\lambda_D}{2\hbar}\right)$, and $\lambda_p = \ln\left(\frac{mv\lambda_D}{\hbar}\right)$, and the Debye length $\lambda_D = \sqrt{kT/(8\pi n_e e^2)}$ (a factor $1/\sqrt{2}$ accounts for ions and electrons with the same T). $\Delta\lambda = \lambda_p - \lambda_{ni}$, and $\lambda_{ni/j} = \ln\left(\frac{\beta\gamma}{2.05\alpha_f Z_{i/j}^{1/3}}\right)$, and $Z_{i/j}$ is the atomic number, and $\alpha_f = 1/137$. The angular brackets indicate a bounce average.

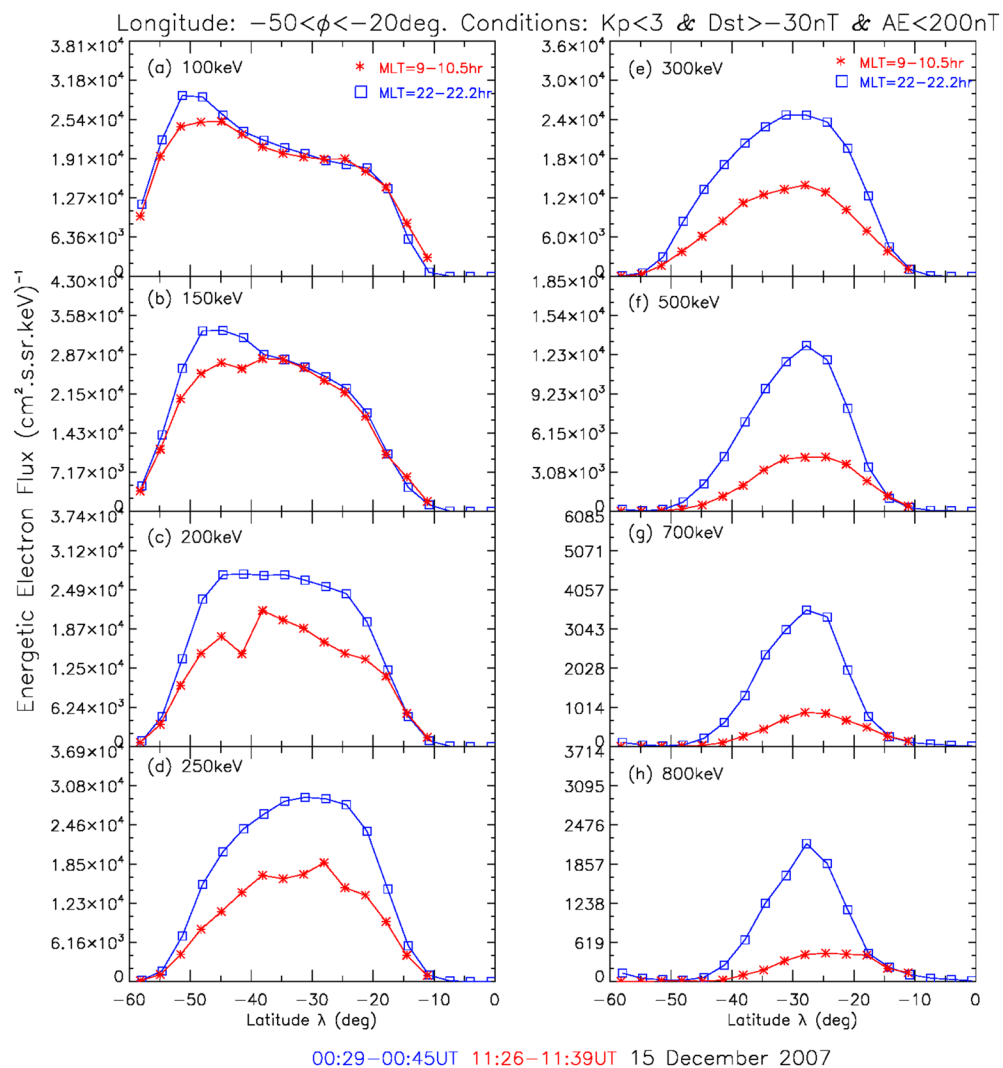


Figure 5. Similar to Figure 2, but around the winter solstice (15 December 2007) during quiet times.

Here, we only calculated the local pitch angle diffusion rate ($D_{\alpha\alpha} = D_{xx}/y^2$ in s⁻¹) of energetic electrons and their loss time ($\tau = 1/(24 \times 3,600 D_{\alpha\alpha})$ in day) at different latitudes. The density and temperature of plasma species (e^- , O^+ , He^+ , H^+) were measured by DEMETER, while the density of neutral atmospheric compositions was calculated with the NRLMSISE-00 atmospheric model (Picone et al., 2002).

Figures 7 and 8 show the loss times of the 100- and 500-keV electrons caused by their collisions with cold plasmas and neutral compositions at 670 km. In most region of the SAA (inside the red closed curves), the collision loss time of the 100-keV electrons is less than half a day ($\tau \leq 0.5$ day in Figure 7), whereas that of the 500-keV electrons is longer than 1 day (Figure 8). The loss time of the 100-keV electrons in the SAA region is comparable to their bounce-averaged drift periods (the drift periods of the lower-energy electrons (<200 keV) are longer than 4.1 hr in Figure 1d). The fast collisions break the drift motion of the lower-energy electrons at 670 km. However, the collision loss time of the 500-keV electrons is longer than longer than their drift periods (the drift periods of the higher-energy electrons (>200 keV) are short than 4.1 hr in Figure 1d). Thus, the higher-energy electrons can maintain their drift motions at 670 km.

In the case of faster drift motions, the slower collision losses cannot result in the day-night difference of the higher-energy electrons (>200 keV), unless the drift orbits of charged particles are originally asymmetrical on the dayside and nightside. Although the lower-energy electrons (<200 keV) undergo faster collision

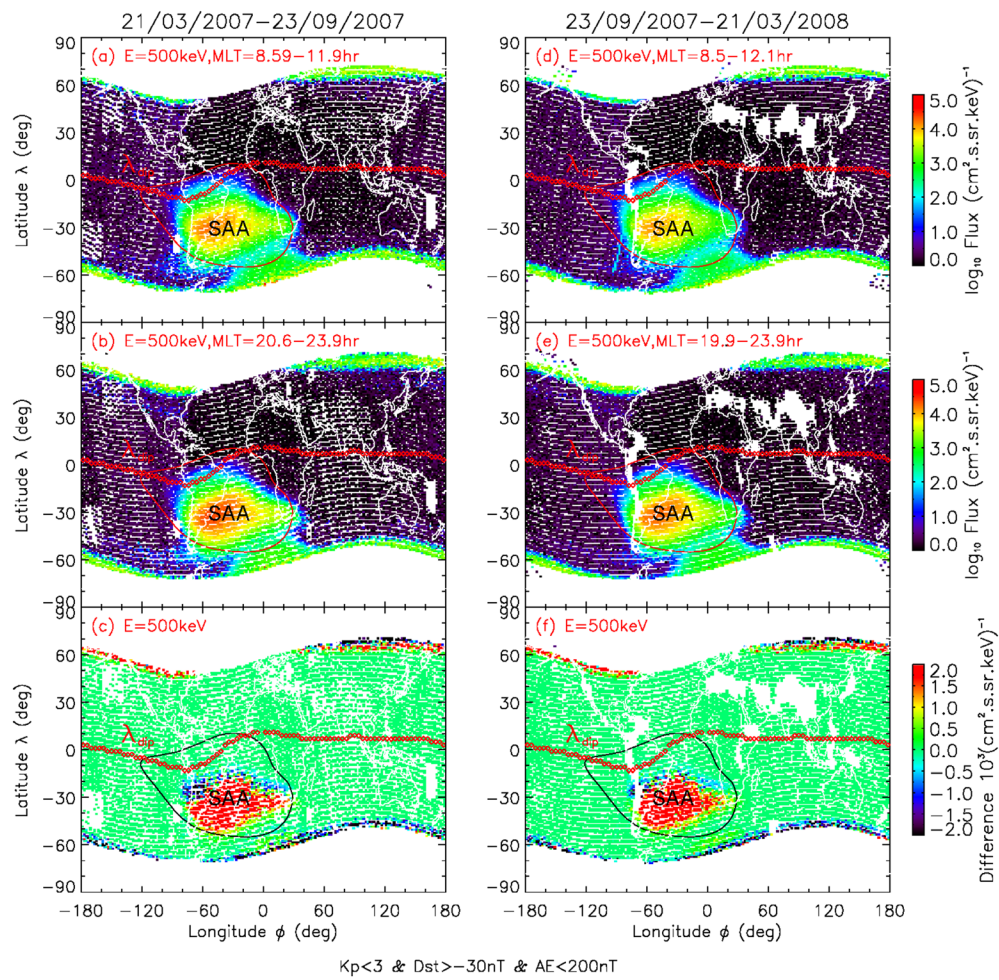


Figure 6. The global distributions of the 500-keV electrons in the daytime and nighttime and their day-night differences at 670 km during quiet times. Difference is equal to the nighttime electron flux minus the daytime one. The South Atlantic Anomaly (SAA) region is marked out by the closed black curves.

losses, their comparable fluxes in the daytime and nighttime suggest that the lower-energy electrons have almost the same sources at different local times, such as a constant source from CRAND (Li, Selesnick, et al., 2017; Selesnick, 2015).

5.2. Effect of the Day-Night Asymmetry of the Drift Shells of Energetic Electrons

To examine the effect of the drift shell splitting on the energetic electrons in SAA region, we simulated the drift orbits of energetic electrons with the magnetic field models of IGRF plus TS04D (aka TS05) (Tsyganenko & Sitnov, 2005). Figure 9 displays the drift orbits of the 85° pitch angle electrons encountered by the DEMETER satellite during quiet times ($Dst \sim H_{SYM} \sim -5$ nT) on 06 June 2007 at 670 km.

During quiet times, the azimuthal drift motions of charged particles are nearly along a magnetic shell with the same magnetic field strength (B). The magnetic field strength (B) decreases with altitude (L). At the same altitude, the magnetic field strength is generally greater on the dayside than the nightside because of the stronger compression of the dayside magnetosphere by high-speed plasma flows in solar wind (Yu et al., 2016). To maintain the equal- B shell drifting, the drift orbits of energetic electrons on the dayside are higher than the nightside in the day-night asymmetric magnetic fields (Li et al., 2016). Therefore, the energetic electrons encountered by DEMETER at 670 km at LT = 10:30 a.m. come from the night side region below 670 km, as indicated by the blue drift orbit. On the contrary, the energetic electrons encountered by DEMETER at 670 km at LT = 10:30 p.m. can drift to the dayside higher altitude (>670 km), as indicated by

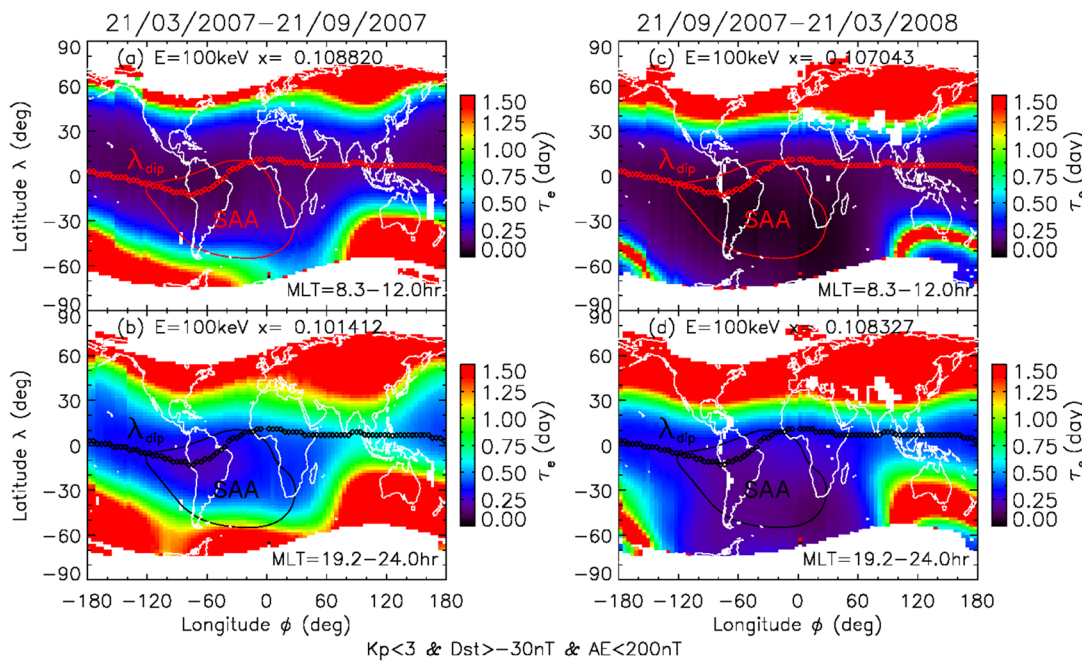


Figure 7. The loss time of the 100-keV electrons caused by their collisions with high-density plasmas and neutral atmospheric compositions at 670 km.

the red drift orbit. Since the fluxes of energetic electrons increase with increasing altitude (L) near the inner edge of the inner radiation belt (Selesnick et al., 2016), the DEMETER satellite encounters more energetic electrons on the nightside than the dayside at the same altitude (~670 km) during quiet times. The day-night asymmetry of the electron's drift orbits and the positive radial gradient of the electron phase space density (i.e., flux increases with L) lead to the day-night difference of the >200 keV electrons in the SAA region at 670 km.

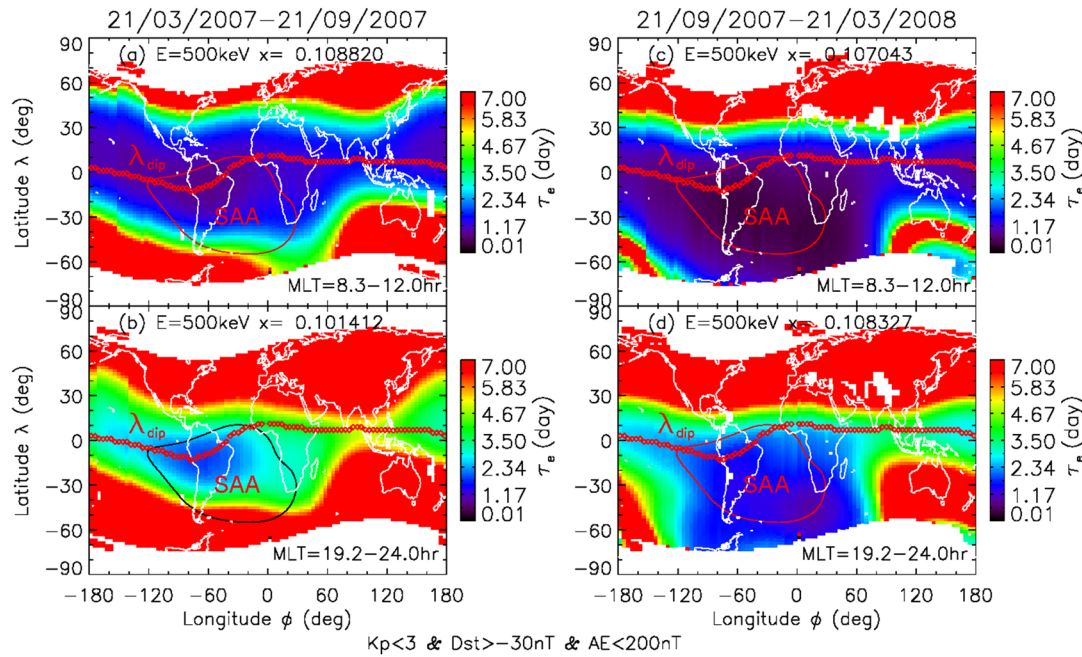


Figure 8. Similar to Figure 7, but for the 500-keV electrons.

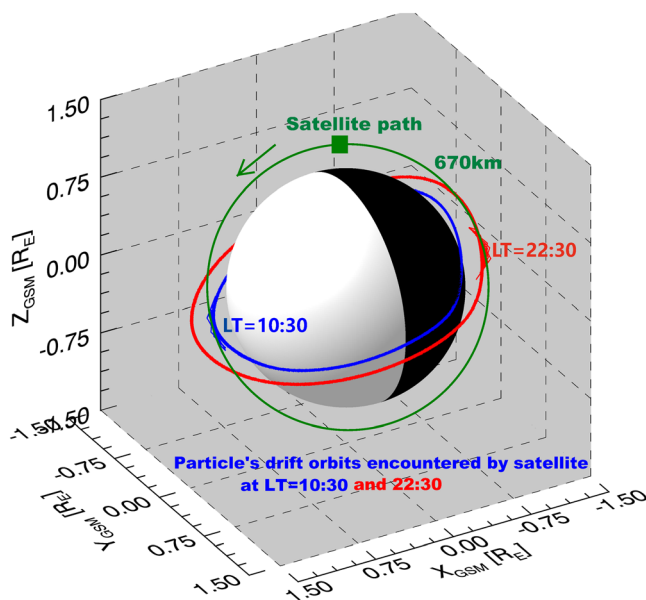


Figure 9. Drift orbits of the 85° pitch angle electrons encountered by DEMETER satellite at different local times at 670 km. Blue and red curves denote the Particle's drift orbits encountered by the satellite at LT = 10:30 a.m. and 10:30 p.m., respectively.

could also change the drift orbits of charged particles and the day-night difference of the higher-energy electrons. The storms and substorms can remarkably change the relativistic electron population in the outer radiation belt ($L > 2$) (Li et al., 2009).

Figures 10 and 11 display the differential fluxes of the 100 to 800 keV electrons at 670 km around the vernal equinox (18 March) and summer solstice (06 June) during active times ($K_p > 3$ or $Dst < -30$ nT or $AE > 200$ nT). In comparison with the electron fluxes during quiet times in the same seasons (Figures 2 and 3), enhanced geomagnetic activities mainly lead to the flux enhancement of energetic electrons in the morning in the SAA region (Figures 10 and 11), whereas the electron fluxes in the nighttime do not increase and even decrease during active times. The inconsistent electron responses at different local times finally weaken the day-night difference of higher-energy electrons (>200 keV) and even cause the higher electron fluxes in daytime but lower fluxes in nighttime at low latitudes ($|\lambda| < 20$ deg, as indicated by Figure 10). During active times, the fluxes of the lower-energy electrons (<200 keV) are larger in the morning than the nighttime at most latitudes.

The electron flux enhancements observed by DEMETER (at $L \sim 1.11$) in morning are consistent with the Van Allen Probes (MagEIS) observations at higher altitudes ($L \sim 1.24$ to 1.3) (Selesnick et al., 2016). The flux enhancement of the 100- to 400-keV electrons on the dawn side are due to the large-scale convection electric field during magnetic storms (Selesnick et al., 2016). The similar electron responses indicate that the enhanced convection electric field also modifies energetic electrons in the SAA region at 670 km. Here, our observations demonstrate for the first time that the day-night difference of energetic electrons in the SAA region depends on electron energy and geomagnetic conditions.

However, it is not yet clear whether high-energy protons have a day-night difference in the SAA region. In the Earth's radiation belts, the fluxes of different-species charged particle depend on the competition between their source and loss (Li, Selesnick, et al., 2017; Li, Yu, et al., 2017). Different sources and loss processes perhaps lead to the different responses of high-energy electrons and protons to magnetic storms. The Van Allen Probes observations indicate that magnetic storms lead to the increase of energetic electrons in the innermost radiation belt ($L \leq 1.3$) on the dawn side (Selesnick et al., 2016). In contrast, other storms also reduce high-energy protons (tens of MeV) in the inner radiation belt and the SAA region, probably owing to the field line curvature scattering or collision losses (Zou et al., 2011, 2015).

The day-night asymmetry of the radiation belt electrons depends not only on the day-night asymmetry of magnetic fields but also on the radial gradient of the electron phase space density. As the radial gradient of the phase space density of energetic electrons is different in different regions of Earth's radiation belts, the day-night asymmetry of electron fluxes is also changed at different altitudes. For example, outside the heart of the outer radiation belt ($L > 5.5$), the fluxes of energetic electrons decrease with altitude (L). In the region of a negative radial gradient of the electron phase space density, the day-strong and night-weak magnetic fields lead to the higher electron fluxes on the dayside than the nightside at the same altitude (e.g., at $L \sim 6.6$) (Li et al., 2013), because the dayside energetic electrons near the outer boundary of the outer radiation belt come from the nightside lower L region with higher fluxes. Besides the influence of the day-night asymmetry of particle's drift orbits, the fluxes of energetic electrons sometimes depend on intensity of electromagnetic waves and local plasma environments (Li et al., 2005, 2008, 2019; Li, Selesnick, et al., 2017; Li, Yu, et al., 2017; Yu et al., 2015).

5.3. Effect of Geomagnetic Activities on Energetic Electrons in SAA Region

Although the higher-energy electrons (>200 keV) can maintain their drift motions during quiet times, their drift shells/motions are probably changed during geomagnetic activities. Since magnetic storms (Dst index) can effectively alter geomagnetic fields (Tsyganenko & Sitnov, 2005), they

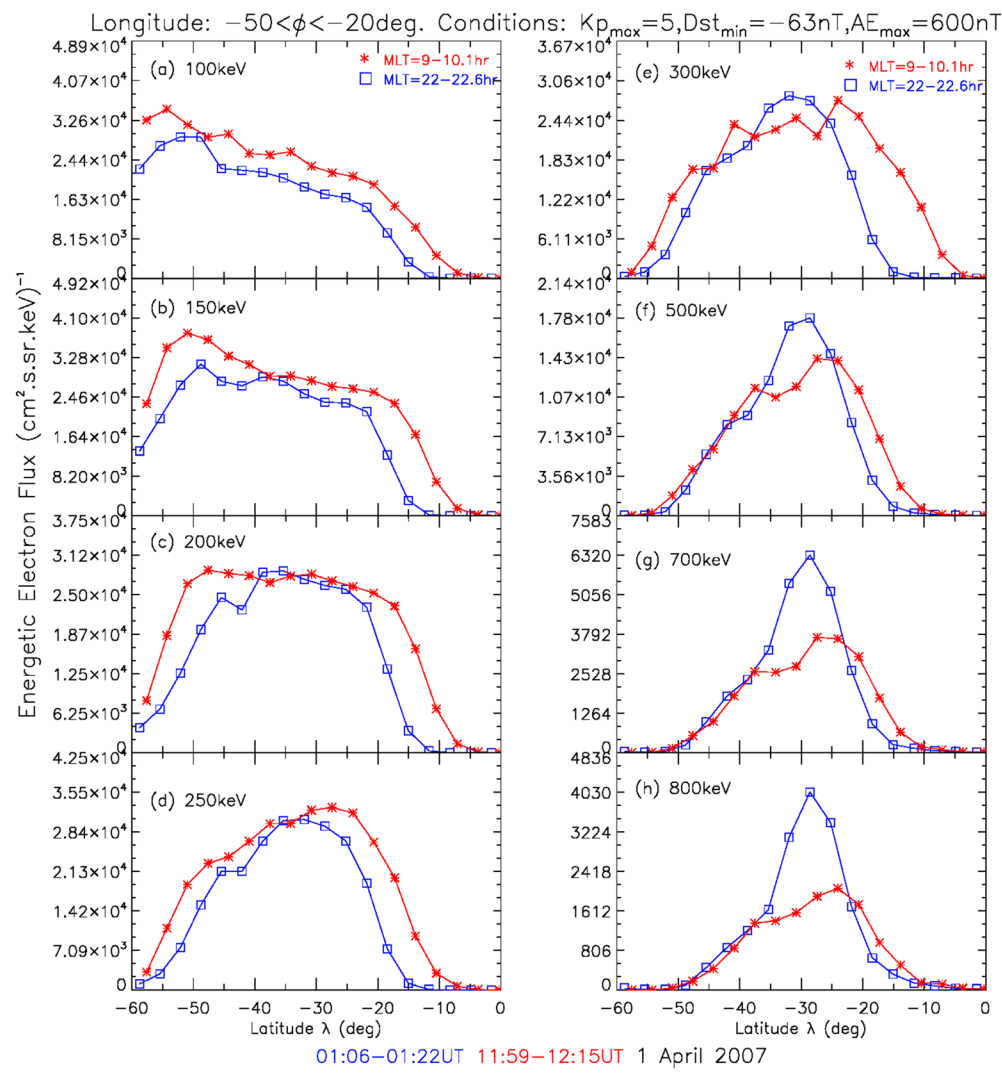


Figure 10. Similar to Figure 2, but around the vernal equinox (01 April 2007) during active times.

6. Summary

By comparing the energetic electron fluxes in SAA region in morning and nighttime in different seasons, we found that the fluxes of higher-energy electrons (>200 keV) are usually larger in the nighttime than the morning in the core region of the SAA during quiet times. However, the fluxes of lower-energy electrons (<200 keV) have no significant day-night difference in the same region. The day-night difference of the energetic electrons in SAA region depends not only on the electron energy but also on the geomagnetic activity levels.

During active times, the fluxes of all energetic electrons increase in the core region of the SAA in the morning, whereas the electron fluxes do not increase and even decrease in the nighttime. Enhanced geomagnetic activities weaken the day-night difference of the higher-energy electrons and even cause the higher electron fluxes in morning at low latitudes ($|\lambda| < 20$ deg). The fluxes of the lower-energy electrons are larger in the morning than the nighttime at most latitudes during active times.

Using the plasma data measured by DEMETER and the neutral densities from the NRLMSISE-00 atmospheric model, we estimated the loss time of energetic electrons due to their collisions with cold plasmas and neutral compositions. The collisions break the drift motion of lower-energy electrons (<200 keV), whereas the higher-energy electrons (>200 keV) can maintain their drift motions at 670 km. During quiet

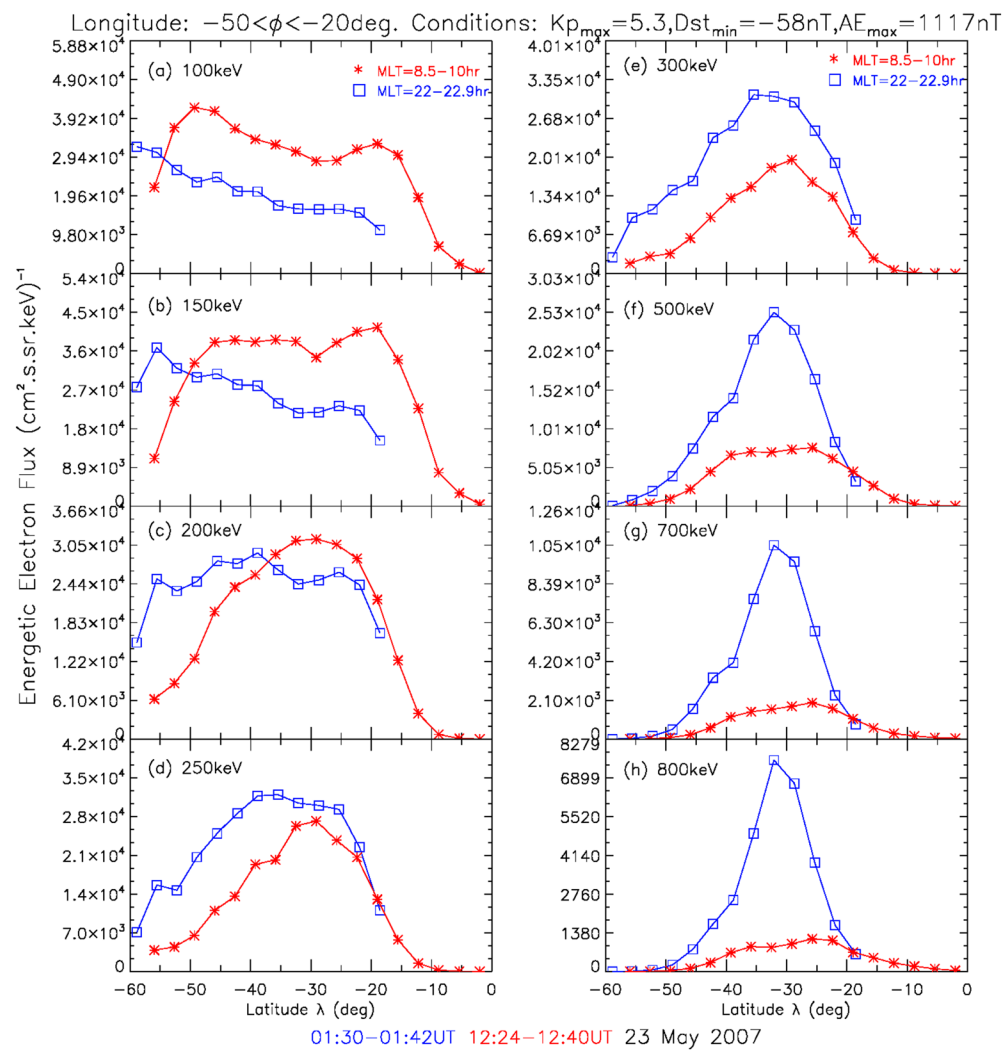


Figure 11. Similar to Figure 3, but around the summer solstice (23 May 2007) during active times.

times, the day-night asymmetry of the electron's drift orbits causes the day-night different electron fluxes in the SAA region near the inner edge of the inner radiation belt, where the fluxes of energetic electrons increase with altitude (L). However, the day-night asymmetry of the electron's drift orbits and the day-night difference of electron fluxes are remarkably changed during active times. The enhanced geomagnetic activities not only increase the energetic electrons in morning but also change the particle's drift orbits and thus break the quiet-time day-night difference of higher-energy electrons.

Data Availability Statement

DEMETER IDP/IAP data are available at the Web site (<http://demeter.cnrsorleans.fr>). Geomagnetic indices (Kp, Dst, and AE) are publicly available from the OMNI database in the CDAWeb (http://cdaweb.gsfc.nasa.gov/sp_phys). We thank all staffs working for these data.

Acknowledgments

This work is supported by National Natural Science Foundation of China (41874192, 41431071, 41374165, and 41074119).

References

- Baker, D. N., Erickson, P. J., Fennell, J. F., Foster, J. C., Jaynes, A. N., & Verronen, P. T. (2018). Space weather effects in the Earth's radiation belts. *Space Science Reviews*, 214(1), 17. <https://doi.org/10.1007/s11214-017-0452-7>
- Berthelier, J. J., Godefroy, M., Leblanc, F., Seran, E., Peschard, D., Gilbert, P., & Artru, J. (2006). IAP, the thermal plasma analyzer on DEMETER. *Planetary and Space Science*, 54(5), 487–501.
- Heirtzler, J. R. (2002). The future of the South Atlantic anomaly and implications for radiation damage in space. *Journal of Atmospheric and Solar-Terrestrial Physics*, 64(16), 1701–1708.

- Horvath, I., & Lovell, B. C. (2009). Distinctive plasma density features of the topside ionosphere and their electrodynamics investigated during southern winter. *Journal of Geophysical Research*, 114, A01304. <https://doi.org/10.1029/2008JA013683>
- Li, L., Cao, J., & Zhou, G. (2005). Combined acceleration of electrons by whistler-mode and compressional ULF turbulences near the geosynchronous orbit. *Journal of Geophysical Research*, 110, A03203. <https://doi.org/10.1029/2004JA010628>
- Li, L. Y., Cao, J. B., Yang, J. Y., Berthelier, J. J., & Lebreton, J.-P. (2015). Semiannual and solar activity variations of daytime plasma observed by DEMETER in the ionosphere-plasmasphere transition region. *Journal of Geophysical Research: Space Physics*, 120, 10,640–10,653. <https://doi.org/10.1002/2015JA021102>
- Li, L. Y., Cao, J. B., Yang, J. Y., & Dong, Y. X. (2013). Joint responses of geosynchronous magnetic field and relativistic electrons to external changes in solar wind dynamic pressure and interplanetary magnetic field. *Journal of Geophysical Research: Space Physics*, 118, 1472–1482. <https://doi.org/10.1002/jgra.50201>
- Li, L. Y., Cao, J. B., & Zhou, G. C. (2008). Whistler-mode waves modify the high-energy electron slot region and the outer radiation belt. *Chinese Journal of Geophysics*, 51, 316–324.
- Li, L. Y., Cao, J. B., Zhou, G. C., & Li, X. (2009). Statistical roles of storms and substorms in changing the entire outer zone relativistic electron population. *Journal of Geophysical Research*, 114, A12214. <https://doi.org/10.1029/2009JA014333>
- Li, L. Y., Yang, J. Y., Cao, J. B., Lu, L., Wu, Y., & Yang, D. M. (2011). Statistical backgrounds of topside-ionospheric electron density and temperature and their variations during geomagnetic activity. *Chinese Journal of Geophysics*. (in Chinese), 54(10), 2437–2444. <https://doi.org/10.3969/j.issn.0001-5733>
- Li, L. Y., Yang, S. S., Cao, J. B., Yu, J., Luo, X. Y., & Blake, J. B. (2019). Effects of solar wind plasma flow and interplanetary magnetic field on the spatial structure of earth's radiation belts. *Journal of Geophysical Research: Space Physics*, 124, 10,332–10,344. <https://doi.org/10.1029/2019JA027284>
- Li, L. Y., Yu, J., Cao, J. B., Wang, Z. Q., Yu, Y. Q., Reeves, G. D., & Li, X. (2016). Effects of ULF waves on local and global energetic particles: Particle energy and species dependences. *Journal of Geophysical Research: Space Physics*, 121, 11,007–11,020. <https://doi.org/10.1002/2016JA023149>
- Li, L. Y., Yu, J., Cao, J. B., Yang, J. Y., Li, X., Baker, D. N., et al. (2017). Roles of whistler mode waves and magnetosonic waves in changing the outer radiation belt and the slot region. *Journal of Geophysical Research: Space Physics*, 122, 5431–5448. <https://doi.org/10.1002/2016JA023634>
- Li, X., Selesnick, R., Schiller, Q., Zhang, K., Zhao, H., Baker, D. N., & Temerin, M. A. (2017). Measurement of electrons from albedo neutron decay and neutron density in near-Earth space. *Nature*, 552(7685), 382–385. <https://doi.org/10.1038/nature24642>
- Lyons, L. R., & Williams, D. J. (1984). *Quantitative aspects of magnetospheric physics*. Dordrecht/Boston/Lancaster: D. Reidel Publishing Company.
- Picone, J. M., Hedin, A. E., Drob, D. P., & Aikin, A. C. (2002). NRLMSISE-00 empirical model of the atmosphere: Statistical comparisons and scientific issues. *Journal of Geophysical Research*, 107(A12), 1468. <https://doi.org/10.1029/2002JA009430>
- Sauvaud, J. A., Moreau, T., Maggioli, R., Treilhou, J. P., Jacquey, C., Cros, A., et al. (2006). High-energy electron detection onboard DEMETER: The IDP spectrometer, description and first results on the inner belt. *Planetary and Space Science*, 54(5), 502–511. <https://doi.org/10.1016/j.pss.2005.10.019>
- Selesnick, R. S. (2012). Atmospheric scattering and decay of inner radiation belt electrons. *Journal of Geophysical Research*, 117, A08218. <https://doi.org/10.1029/2012JA017793>
- Selesnick, R. S. (2015). High-energy radiation belt electrons from CRAND. *Journal of Geophysical Research: Space Physics*, 120, 2912–2917. <https://doi.org/10.1002/2014JA020963>
- Selesnick, R. S., Su, Y.-J., & Blake, J. B. (2016). Control of the innermost electron radiation belt by large-scale electric fields. *Journal of Geophysical Research: Space Physics*, 121, 8417–8427. <https://doi.org/10.1002/2016JA022973>
- Tsyganenko, N. A., & Sitnov, M. I. (2005). Modeling the dynamics of the inner 542 magnetosphere during strong geomagnetic storms. *Journal of Geophysical Research*, 110, A03208. <https://doi.org/10.1029/2004JA010798>
- Ye, Y., Zou, H., Zong, Q., Chen, H., Wang, Y., Yu, X., & Shi, W. (2017). The secular variation of the center of geomagnetic South Atlantic Anomaly and its effect on the distribution of inner radiation belt particles. *Space Weather*, 15, 1548–1558. <https://doi.org/10.1002/2017SW001687>
- Yu, J., Li, L. Y., Cao, J. B., Reeves, G. D., Baker, D. N., & Spence, H. (2016). The influences of solar wind pressure and interplanetary magnetic field on global magnetic field and outer radiation belt electrons. *Geophysical Research Letters*, 43, 7319–7327. <https://doi.org/10.1002/2016GL069029>
- Yu, J., Li, L. Y., Cao, J. B., Yuan, Z. G., Reeves, G. D., Baker, D. N., et al. (2015). Multiple loss processes of relativistic electrons outside the heart of outer radiation belt during a storm sudden commencement. *Journal of Geophysical Research: Space Physics*, 120, 10,275–10,288. <https://doi.org/10.1002/2015JA021460>
- Zhang, K., Li, X., Zhao, H., Schiller, Q., Khoo, L.-Y., Xiang, Z., et al. (2019). Cosmic ray albedo neutron decay (CRAND) as a source of inner belt electrons: Energy spectrum study. *Geophysical Research Letters*, 46, 544–552. <https://doi.org/10.1029/2018GL080887>
- Zou, H., Li, C., Zong, Q., Parks, G. K., Pu, Z., Chen, H., et al. (2015). Short-term variations of the inner radiation belt in the South Atlantic anomaly. *Journal of Geophysical Research: Space Physics*, 120, 4475–4486. <https://doi.org/10.1002/2015JA021312>
- Zou, H., Zong, Q. G., Parks, G. K., Pu, Z. Y., Chen, H. F., & Xie, L. (2011). Response of high-energy protons of the inner radiation belt to large magnetic storms. *Journal of Geophysical Research*, 116, 201–208. <https://doi.org/10.1029/2011JA016733>